IOP Publishing Journal of Physics: Condensed Matter
J. Phys.: Condens. Matter **26** (2014) 464109 (13pp) doi:10.1088/0953-8984/26/46/464109

# First-order phase transition during displacement of amphiphilic biomacromolecules from interfaces by surfactant molecules

**Rammile Ettelaie[1], Eric Dickinson[1] and Luis Pugnaloni[2]**

[1] Food Colloids Group, School of Food Science and Nutrition, University of Leeds, Leeds LS2 9JT, UK
[2] Departamento de Ingeniería Mecánica, Facultad Regional La Plata, Universidad Tecnológica Nacional, 1900 La Plata, Argentina

E-mail: r.ettelaie@leeds.ac.uk

Received 11 March 2014, revised 10 April 2014
Accepted for publication 11 April 2014
Published 27 October 2014

**Abstract**

The adsorption of surfactants onto a hydrophobic interface, already laden with a fixed number of amphiphilic macromolecules, is studied using the self consistent field calculation method of Scheutjens and Fleer. For biopolymers having unfavourable interactions with the surfactant molecules, the adsorption isotherms show an abrupt jump at a certain value of surfactant bulk concentration. Alternatively, the same behaviour is exhibited when the number of amphiphilic chains on the interface is decreased. We show that this sudden jump is associated with a first-order phase transition, by calculating the free energy values for the stable and the metastable states at both sides of the transition point. We also observe that the transition can occur for two approaching surfaces, from a high surfactant coverage phase to a low surfactant coverage one, at sufficiently close separation distances. The consequence of this finding for the steric colloidal interactions, induced by the overlap of two biopolymer + surfactant films, is explored. In particular, a significantly different interaction, in terms of its magnitude and range, is predicted for these two phases. We also consider the relevance of the current study to problems involving the competitive displacement of proteins by surfactants in food colloid systems.

Keywords: mixed surfactant + biopolymer films, first-order phase transition, colloidal steric interactions

(Some figures may appear in colour only in the online journal)

## 1. Introduction

Colloidal formulations of importance in many technological applications, including inks and paints, personal care products, agrochemicals, pharmaceuticals, and above all foods, often contain a multitude of different surface active molecules [1–3]. For example, in food emulsions, lecithin, monoglycerides, Tweens and other similar low molecular weight surface active molecules, are frequently present as emulsifiers [3]. These serve to reduce the oil–water interfacial tension thus facilitating the breakup of oil droplets. Their relatively small size also results in fast adsorption kinetics, again an attribute of some importance when producing fine emulsions. At the same time, these systems also contain macromolecules such as proteins and other biopolymers, which act as steric and electrostatic stabilisers and are necessary to prevent the coalescence of the droplets and ensure the long term colloidal stability of the emulsion product [1, 2, 4]. The simultaneous presence of several different surface active species gives rise to a number of interfacial related phenomena, only seen in such mixed systems [5–9]. An obvious example is the competitive adsorption, leading to a gradual displacement of one surface

 © 2014 IOP Publishing Ltd Printed in the UK

active species by the other from the interface. Recent experimental [6, 10–13] and computer simulation studies [14–16], considering the displacement of proteins by smaller surfactant molecules at air–water and oil–water interfaces, have revealed that the process progresses in a rather non-homogeneous manner. During the displacement kinetics, sometimes referred to as the orogenic displacement mechanism, islands of displaced protein with complex morphologies are formed [5, 6, 14].

The presence of two or more surface active species also gives rise to the formation of mixed interfacial adsorbed layers. The structure and composition of these layers is sensitive to the strength and nature of the interactions that might exist between different constituent molecules. In particular, the unfavourable interactions between different species can lead to the possibility of a structural phase transition, as well as phase separation behaviour in the interfacial film. However, one aspect of the phase separation behaviour at the interfaces, differentiating it from the more usual case occurring in the bulk, is that an adsorbed surface layer is always in contact with two or more bulk sub-phases. Different surface active molecules, depending on conformational changes they undergo during desorption, their adsorption energies, size, diffusion coefficient and solubility, may or may not be able to exchange rapidly enough with the bulk phase during the experimental time scales. Thus, two limiting kinds of behaviour can be envisaged. In the first, a particular surface active species adsorbed at the interface maintains the same chemical potential and is at equilibrium with the bulk phase at all times. In the second case, the molecules can be considered as being irreversibly adsorbed at the interface so that the overall surface coverage, set by the initial conditions, is maintained at a fixed value throughout the duration of the experiment.

As has been argued previously by us [17, 18] that, whenever all adsorbed species are at equilibrium with the bulk sub-phase (or sub-phases), no phase separation phenomenon can occur at the interface. This follows from the fact that in such systems no restrictions on the composition of the adsorbed layers are imposed. Thus, rather than separating into two or more distinct regions, the interface, through adsorption and desorption of the appropriate molecules, can evolve and adopt the composition which has the lowest free energy. More formally, for a system containing two competing amphiphilic type molecules A and B, the surface coverage of the species, $\Gamma_a$ and $\Gamma_b$, will be determined by the set of equations $\mu_a(\Gamma_a, \Gamma_b) = \mu_a^{bulk}$ and $\mu_b(\Gamma_a, \Gamma_b) = \mu_b^{bulk}$. The quantities $\mu_a$ and $\mu_b$ denote the chemical potentials of the adsorbed molecules A and B at the interface. For a given temperature and a fixed set of external parameters, these are only functions of the surface coverage of the two species. Similarly, we denote the chemical potentials of A and B in the bulk solution as $\mu_a^{bulk}$ and $\mu_b^{bulk}$, respectively. These latter quantities are set by the concentration of the two species specified by the initial experimental conditions. It may be argued that, under certain special conditions, the above set of equations may admit more than one set of solutions for ($\Gamma_a$, $\Gamma_b$). In such cases, it is possible in principle to have coexisting regions on the interface with different surface coverage compositions. However, in practice the existence of a line tension between these different surface patches means that one of the phases will eventually prevail and once again the equilibrium coverage at the interface is expected to be a uniform one. Of course, it is also assumed that for such systems the concentration of the individual species in the bulk is sufficiently low so as not to cause any bulk phase separation.

The above situation is in stark contrast to the opposite case where none of the species initially placed at the interface has time to exchange with the bulk sub-phase. For these systems, the existence of sufficiently strong unfavourable interactions between the two surface active species can result in surface phase separation.

If the surface coverage of A and B molecules in each of the two separate phases 1 and 2 is ($\Gamma_a^{(1)}$, $\Gamma_b^{(1)}$) and ($\Gamma_a^{(2)}$, $\Gamma_b^{(2)}$), then the equilibrium condition demands that $\mu_a(\Gamma_a^{(2)}, \Gamma_b^{(2)}) = \mu_a(\Gamma_a^{(1)}, \Gamma_b^{(1)})$ and $\mu_b(\Gamma_a^{(2)}, \Gamma_b^{(2)}) = \mu_b(\Gamma_a^{(1)}, \Gamma_b^{(1)})$. Furthermore, the fixed total number of each surface active species at the interface now implies that $\alpha\Gamma_a^{(1)} + (1-\alpha)\Gamma_a^{(2)} = \Gamma_a^{total}$ and $\alpha\Gamma_b^{(1)} + (1-\alpha)\Gamma_b^{(2)} = \Gamma_b^{total}$, where the overall coverage values, $\Gamma_a^{total}$ and $\Gamma_b^{total}$ are set by the amount of each molecule A and B placed initially at the interface. The fraction of the surface with a composition ($\Gamma_a^{(1)}$, $\Gamma_b^{(1)}$) is denoted here as $\alpha$. In defining the coverage values, as is customary, we have taken the Gibbs dividing plane [19, 20] such that the net excess solvent at the interface is always zero. The above four equations, together with the requirement for the free energy of the interface to be minimum dictates the values of $\alpha$, $\Gamma_a^{(1)}$, $\Gamma_b^{(1)}$,$\Gamma_a^{(2)}$ and $\Gamma_b^{(2)}$. Although not necessarily always the case for the mixtures of two amphiphilic molecules at interfaces, the additional constraint that $\Gamma_a^{(1)} + \Gamma_b^{(1)} = \Gamma_a^{(2)} + \Gamma_b^{(2)} =$ constant, reduces the procedure to the familiar 'lever rule' for identifying the composition of the two phases and their abundance on the surface. Qualitatively, the situation is now similar to the competitive phase separation behaviour seen in bulk systems. Surface phase separation behaviour of this type has been the subject of many experimental and theoretical studies in recent years [21–26].

It is important to realise that the incompatibility between different surface active species need not necessarily be the result of direct unfavourable forces between the constituent molecules. Using Brownian dynamics simulations, we have shown that incompatibility can also arise from the formation of reversible bonds amongst one set of molecules, but not the other [17]. Formation of such reversible bonds results in an effective attraction between the bond forming molecules, sufficient to induce phase separation. The same phenomenon has also been predicted theoretically and demonstrated experimentally for mixtures of two very similar set of polymers [27–29]. In these studies the two sets of polymers were chemically very similar, with one set only slightly modified by attachment of small hydrophobic groups at the two ends of the chains. These serve to produce weak reversible bonds, driven by hydrophobic forces, between the modified molecules, but not the unmodified ones. As a result, it is observed that the mixed solution breaks up into two distinct phases, one rich in the associating molecules and the other in unmodified ones [27–30]. We also suspect that the possible surface phase separation reported for certain mixed protein films occurring

at air–water interfaces [31–35] is also the result of a very similar mechanism.

A third and less frequently studied scenario, intermediate between the two cases discussed above, can also be envisaged. Here, whilst one of the surface active components is rapidly exchanging with the bulk, the other has a fixed overall surface coverage. Once again, in food colloids such a situation is commonplace, as both low molecular weight surfactants and amphiphilic biopolymers are often present together [36, 37]. Interfacial dynamic measurements suggest that the time scale for adsorption-desorption kinetics of some food protein molecules can be several hours long [38–41]. For low molecular weight surfactants, this time is typically between a few seconds down to a few milliseconds [42–44]. Using analytical mean field calculations and Monte Carlo simulations, we have considered phase separation behaviour in a simple tertiary A + B + solvent lattice model [18]. In this model, two of the components, the A and the solvent molecules, could alter their surface coverage. The third component, however, was constrained to have a fixed concentration. As the unfavourable interaction between the A and B surface active species was made stronger, a two phase region emerged. As expected, for a fixed adsorption energy of the A component, the extent of the phase separated region in the phase diagram broadens with the strength of the unfavourable A–B interaction. However more interestingly, and in clear contrast to the phase separation in systems with a fixed overall composition, it is found that the region in which the separation occurs through spinodal decomposition becomes narrower as the incompatibility between A and B is increased. In other words, for strongly incompatible surface active species, the phase separation at the interface is most likely to proceed by the nucleation and growth mechanism.

The simple model studied by us [18] took no account of different internal configurations adopted by the adsorbed molecules. The availability of a large number of internal states is an important feature of large macromolecules. In the present work, we use the self consistent field calculation (SCF) scheme of Scheutjens and Fleer [45–47] to study the behaviour of irreversibly adsorbed macromolecules, in the presence of competing surfactants that can freely exchange with the bulk. The model presented is also relevant to synthetic, polymer grafted surfaces, which in many process operations come into contact with surfactant solutions. We discuss the possibility of the existence of a first-order phase transition in this system, e.g. as manifest through a discontinuity in the adsorption isotherm for the surfactant, when the unfavourable interactions between hydrophobic sections of surfactants and polymer chains are sufficiently strong.

A variety of different kinds of structural phase transition behaviour in brushes, consisting of polymeric chains anchored or strongly adsorbed to surfaces, has been reported in the literature over the past few decades. One of the best known cases is the so called mushroom–brush transition [47, 48], seen in grafted surfaces in contact with a good or a theta solvent. At low grafting densities the non-overlapping chains adopt a coil-like configuration, with dimensions similar to those of the free polymer in the corresponding solvent. As the grafting density is increased, the chains begin to stretch in order to reduce the degree of overlap with their neighbouring chains. The balance between this factor and the opposing loss of entropy due to stretching determines the thickness of the brush. A somewhat related case involves anchored polymers with a certain degree of adsorption affinity to the surface. At low grafting densities, chains lie flat on the surface to optimise the number of polymer–surface contacts. At a higher grafting coverage, the surface becomes saturated and the overlap between the chains causes stretching of the polymers into the solution. It has been speculated that this pancake–brush transition might be a first-order transition [49]. However, as with the mushroom–brush case, detailed numerical SCF calculations by Currie *et al* [50]. have shown that the transition remains a continuous one for finite size chains, at finite segment adsorption energies. Only as the strength of attractive segment-surface interaction, $\chi_s$, becomes infinite does a discontinuous transition result [50]. It is interesting to point out that, in this sense, the pancake–brush transition, exhibited in these systems, can be considered as a zero temperature phase transition (since $\chi_s \sim 1/T$), much in the same way as those predicted in certain models of spin-glasses and other magnetic systems [51]. Skvorsov *et al* [52], using both analytical and numerical SCF calculations, have studied a similar type of behaviour in certain mixed brushes. These brushes consist of non-adsorbing polymers, but with a small addition of longer adsorbing chains. All chains are anchored to the surface at one end. For a fixed chain length ratio, a first-order phase transition is predicted at a given well-defined surface adsorption energy, but only in the limit of infinite chain lengths. For adsorption energies stronger than the critical value, the minority long chains take up a pancake-type conformation, whereas a weaker adsorption results in stretched brush configurations [52]. As a result, at the transition point, the number of contacts between the minority chains and the surface shows an abrupt discontinuity. It is worth pointing out that the phase transition behaviour reported in the current work differs from those mentioned above in that the phase transition is driven by a strong incompatibility between the small surfactant and larger anchored chains. As such, the existence of a first-order phase transition, and the related metastable states, is a feature that emerges even for finite sized chains.

The reminder of the paper is organised as follows. In the next section we give a brief account of the model and the calculation methodology adopted. In section 3 we present our SCF calculation results. We provide evidence for the existence of metastability and a first-order phase transition in grafted polymeric brushes in contact with solutions of competing low molecular weight surface active molecules. These results are extended to cases involving two interfaces in close proximity, in section 4. We note that, for solutions involving solely charged surfactants, a phase transition associated with confinement has already been predicted [53, 54] as two surfaces approach each other. Therefore, also for the systems studied here, the variation in the separation distance between the two surfaces is expected to be yet another parameter that can induce an abrupt transition from one phase to the other. Finally, in section 5 we provide a summary of the main conclusions of the study.

## 2. Methodology

The model studied here consists of a solid–liquid interface with macromolecular chains terminally anchored to the solid surface at one end, at a specified uniform coverage. The chains are amphiphilic, consisting of a single hydrophobic and a single hydrophilic block. From now on we shall refer to the monomer segments making up these blocks as A and B, respectively. While the hydrophobic segments are assumed to have a certain affinity for adsorption onto the interface, the hydrophilic B monomers favour remaining in the aqueous solvent. The solvent itself contains additional small chains, which themselves comprise of a hydrophilic head, made from segments D, and a hydrophobic tail consisting of monomers C. These chains represent the low molecular weight surfactant-like molecules in our model. They have to compete for adsorption onto the surface with the long chains (representing protein) already at the interface, but otherwise are free to exchange between the bulk and the surface. For simplicity, we shall assume that the solvent molecules and monomer types A to D all have the same size, $a_o$.

Following the formalism of Ferreira and Leibler [55] and others [56, 57], the free energy for the above system can be expressed in terms of the following functional integral, taken over all possible density profile variations for each type of monomer segment, $\phi^\alpha(r)$:

$$\Delta F = -k_B T \ln\left( \int \exp(-\beta \Delta f([\phi^\alpha]) \prod_\alpha \mathfrak{D}\phi^\alpha \right) \quad (1)$$

where $\beta = 1/(k_B T)$, $T$ is the temperature and $k_B$ the Boltzmann constant. The functional $\Delta f([\phi^\alpha(r)])$ in the above equation, expresses the free energy per unit area associated with a given non-uniform density profile, up and beyond that for a uniform density distribution of non-anchored species. It is given by

$$\frac{\Delta f}{k_B T} = \sum_i -n_i \ln\left(\frac{Q_i}{Q_i^0}\right) - \sum_\alpha \left[ \int_0^\infty \phi^\alpha(r)\psi^\alpha(r)\, dr \right] + \frac{1}{2}\sum_{\alpha\beta} \int_0^\infty \chi_{\alpha\beta} (\phi^\alpha(r) - \Phi^\alpha)\, (\phi^\beta(r) - \Phi^\beta)\, dr + \sum_\alpha \chi_{\alpha s} \phi^\alpha(0) \quad (2)$$

with the index $i$ running over all molecular species present in the system and summations $\alpha$ and $\beta$ taken over the solvent molecules and segment types A to D. The number of molecules of species $i$ is denoted by $n_i$. The bulk concentration of the segments A and B, $\Phi^A$ and $\Phi^B$, belonging to the terminally anchored chains, is set to zero. As usual, the interactions between different monomer types are assumed to be short ranged and are represented by the set of Flory-Huggins parameters $\chi_{\alpha\beta}$. Similarly, the parameters $\chi_{\alpha s}$ specify the adsorption energies for different segment types, in contact with the solid interface located at $r = 0$. It is convenient to express all distances in units of $a_o$ from now on and also work with number density distributions rather than concentrations. As such, $\Delta f$ in equation (2) is given as per unit area $a_o^2$ and the number densities and volume fractions become identical and can be used interchangeably. We have additionally assumed that the interface is homogeneous and therefore only the variation of the density profiles in the direction perpendicular to the surface needs be considered. Note that equation (2) is not an explicit equation in $\{\phi^\alpha(r)\}$, as it also involves a set of auxiliary fields $\{\psi^\alpha(r)\}$ associated with each monomer kind $\alpha$, such that the functional derivatives are given by [55]

$$-\frac{\delta \sum_i n_i \ln Q_i}{\delta \psi^\alpha(r)} = \phi^\alpha(r) \quad (3)$$

Thus these fields can be thought of as external fields which, when applied to a set of non-interacting free chains (i.e. an identical system but with all $\chi$ parameters set to zero), result in the specified concentration profile $\{\phi^\alpha(r)\}$. The quantities $Q_i$ and $Q_i^o$ denote the single chain partition functions for molecules belonging to species $i$ in the presence and in the absence of these fields, respectively. For non-anchored molecules, including those of the solvent, it can be shown that the first term in (2) can be replaced by the excess interfacial concentration of those species [47]:

$$-n_i \ln\left(Q_i / Q_i^o\right) = -(1/N_i) \int_0^\infty \left(\phi_i(r) - \Phi_i\right)\, dr \quad (4)$$

where the size of the chains of type $i$ is $N_i$. As we are also interested in the nature of colloidal interactions mediated between two surfaces in the above mixed system, it is useful from the onset to consider a situation involving two surfaces at a distance $L$ apart. In this case the integrals in (2) and (4) extend from 0 to $L$. The properties of a single isolated interface can always be calculated, by setting the separation distance $L$ sufficiently large.

As with other mean-field type models, SCF calculations assume that the functional integral in equation (1) is dominated by the density profile that minimises the free energy (2). This density profile, and the subsequent calculation of $Q_i$, is most efficiently achieved through the numerical scheme introduced by Scheutjens and Fleer [45–47, 58] for homopolymers and further extended by Evers *et al* [59, 60] to copolymer systems. In this scheme, one divides the distance between the plates into layers of one (monomer) unit each, from $k = 1$ to $k = L$. It turns out that the density profile minimising the free energy satisfies the following set of conditions [47]

$$\psi^\alpha(k) - \chi_{\alpha s}(\delta_{k0} + \delta_{kL}) - \sum_\gamma \chi_{\alpha\gamma}(\phi^\gamma(k) - \Phi^\gamma) = \psi^\beta(k) - \chi_{\beta s}(\delta_{k0} + \delta_{kL}) - \sum_\gamma \chi_{\beta\gamma}(\phi^\gamma(k) - \Phi^\gamma) \quad (5)$$

for all values of the indices $\alpha$ and $\beta$, when the system is not compressible, i.e. with the additional restriction that $\sum_\gamma \phi^\gamma(k) = 1$ for each layer. The symbol $\delta_{kj}$ in the above expression denotes the usual Kronecker delta function ($\delta_{kj} = 1$ for $k = j$, and $\delta_{kj} = 0$ otherwise). More precisely, the set of equation (5) only ensures a stationary profile with respect to

small fluctuation in the density. In particular, it does not preclude a solution that happens to be a local minimum. In the lattice model formulation of the problem it is customary to allow for interactions between different monomers to extend between adjacent layers too. This can easily be achieved by replacing the $\phi^{\gamma}(k)$ in (5) with its value averaged over three consecutive layers, $<\phi^{\gamma}(k)>$, as defined by

$$<\phi^{\gamma}(k)> = \lambda_{-1}\phi^{\gamma}(k-1)+\lambda_0\phi^{\gamma}(k)+\lambda_{+1}\phi^{\gamma}(k+1) \quad (6)$$

The values of the constants $\lambda_{-1}$, $\lambda_{+1}$ and $\lambda_0$ depend on the underlying lattice chosen for the purpose of the numerical calculations. For the simple cubic lattice adopted here, the corresponding values are $\lambda_{-1} = \lambda_{+1} = 1/6$ and $\lambda_0 = 4/6$. Note that condition (5) implies that the values of the auxiliary fields $\{\psi^{\alpha}(r)\}$ are those which correspond to the mean-fields which will be experienced by the monomers of each type $\alpha$, at location $r$, due to their interactions with the surrounding monomers. However, it should be stressed that this identification of the values of $\{\psi^{\alpha}(r)\}$ with the mean-fields only applies to the set of density profiles that minimises the free energy.

In the usual implementation of the Scheutjens-Fleer scheme [59], (5) is solved through an iterative procedure, starting with a suitable initial guess for the set of auxiliary fields $\{\psi^{\alpha}(r)\}$. The density profiles associated with these fields are next calculated by constructing the end segment distribution functions, $G_i^{(j)}(k, s)$, for the first $s$ segments of the $i^{\text{th}}$ species, at each layer $k$. Since it is possible to consider $s$ monomers from either end of a chain, there will be two complementary ways of defining such an end point distribution function. To distinguish between the two we use the index $j = 1$ or 2. We also define two groups of chain architecture operators $t_{i1}(s)$ and $t_{i2}(s)$ for each species. These simply equate to the type of monomer (A, B, C or D) with the ranking number $s$, counted from the appropriate end of the chain, $j = 1$ or 2. Using the connectivity of the chains, the value of $G_i^{(j)}(k, s)$ is readily obtained using the following recurrence relation:

$$G_i^{(j)}(k, s) = g_{t_j(s)}(k)\Big(\lambda_{-1}G_i^{(j)}(k-1, s-1) + \lambda_0 G_i^{(j)}(k, s-1) + \lambda_1 G_i^{(j)}(k+1, s-1)\Big) \quad (7)$$

where $g_{\alpha}(k)$ denotes the free segment distribution function for monomers of kind $\alpha$ and is simply given by the Boltzmann factor $\exp(-\beta\psi^{\alpha}(k))$, featuring the potential $\psi^{\alpha}(k)$ acting on every such monomer type at layer $k$. To initiate the recurrence equation (7), the value of $G_i^{(j)}(k, 1)$ needs to be specified first. This is set to $G_i^{(j)}(k, 1) = g_{t_{ij}(1)}(k)$, if the molecules are free. However, for chains tethered to the surface, assuming that the anchored end is the one denoted by $j = 1$, we have $G_i^{(1)}(k, 1) = g_{t_{i1}(1)}(k)(\delta_{k1}+\delta_{kL})$. This reflects the fact that the first segments of these molecules can only reside in layers $k = 1$ or $k = L$ which are in contact with the solid surfaces. The final step in the calculation of the density profiles involves the use of the so called compositional law [47, 59]:

$$\phi^{\alpha}(k) = \sum_i \sum_{s=1}^{N_i} C_i \frac{G_i^1(k, s)G_i^2(k, N_i-s+1)}{g_{\alpha}(k)}\,\delta_{t_{i1}(s),\alpha} \quad (8)$$

The normalisation constant, $C_i$, in the above equation can be shown to be $\Phi_i/N_i$ for the free chains [54], while for the anchored chains, with $\Gamma_i$ chains per unit area on each surface, it is given by $2\Gamma_i\left(\sum_{k=1}^{L} G_i^1(k, N_i)\right)^{-1}$. In using this latter equation, we have assumed that our final solution will be a symmetrical one with respect to the two surfaces. This also means that the single chain partition function $Q_i$, referred to in (1), is given as

$$\frac{Q_i}{Q_i^0} = (1/2)\left(\sum_{k=1}^{L} G_i^1(k, N_i)\right) \quad (9)$$

for the tethered chains. With the density profiles for the given values of the auxiliary fields determined, one can now check to see if the condition (5), as well as the incompressibility criteria, are satisfied. The values of the fields are then systematically adjusted and the process is repeated for a sufficient number of iterations until convergence is obtained. The free energy change in the system, resulting from the non-uniform density profile due to the presence of the two surfaces, can be calculated by substituting our solution into the suitably discretised form of (2), appropriate to the underlying lattice one adopts in the numerical computation. The modification also reflects the interactions between adjacent layers, introduced in the discretised lattice scheme, and the presence of a second solid surface at $k = L$. With these additions included, the final expression for the discretised form of (2) becomes [61, 62]

$$\begin{aligned}\frac{\Delta F}{k_BT} = &\sum_i -2\Gamma_i \ln\left(\frac{Q_i}{Q_i^0}\right) - \sum_{k=1}^{L}\sum_j \frac{\left(\phi_j(k)-\Phi_j\right)}{N_j} \\ &- \sum_{k=1}^{L}\sum_a \phi^{\alpha}(k)\psi^{\alpha}(k) \\ &+ \frac{1}{2}\sum_{k=1}^{L}\sum_{\alpha\beta}\chi_{\alpha\beta}(\phi^{\alpha}(k)-\Phi^{\alpha})\,(<\phi^{\beta}(k)>-\Phi^{\beta}) \\ &+ \sum_{\alpha}\chi_{\alpha s}(\phi^{\alpha}(1)+\phi^{\alpha}(L))\end{aligned} \quad (10)$$

where the summation $i$ is taken over all the free species, while that over $j$ involves the anchored chains. The first three terms in the above expression represent the entropic and the last two the enthalpic contributions to the free energy of the system [63].

As well as studies involving the adsorption and interfacial properties of macromolecules in food systems, it should be mentioned that SCF calculations have also been successfully used to predict the bulk self-assembly behaviour and formation of liquid crystalline phases in foods involving biopolymers [64, 65].

## 3. Adsorption onto a single surface

### 3.1. Surfactant surface coverage

In this section we shall consider the adsorption of surfactant molecules, consisting of 6 head and 6 tail segments, onto an otherwise hydrophobic solid surface containing diblock

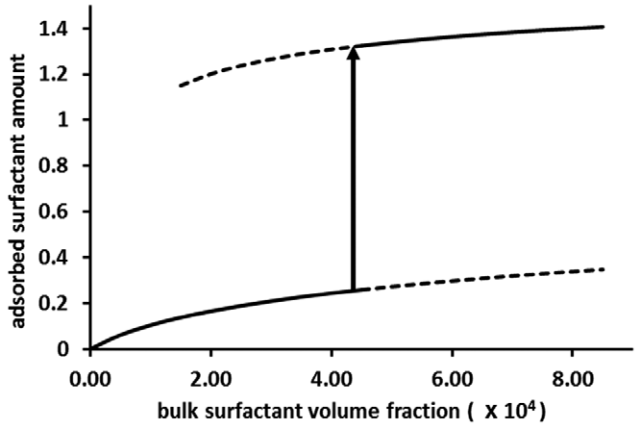


**Figure 1.** Discontinuity in the surfactant adsorption isotherm indicating a first-order phase transition at a bulk surfactant volume fraction of $4.35\times10^{-4}$, highlighted here by the arrow. The amount of adsorbed surfactant is calculated according to (11). The dotted lines correspond to the metastable solutions found for each phase.

polymers. We refer to these segments as (D) and (C) monomers, respectively. As mentioned before, the diblock polymers are also amphiphilic, each consisting of a hydrophobic (A) and a hydrophilic (B) block. Such diblock models are often taken as the simplest first approximation to disordered protein molecules in many theoretical studies [66, 67]. In what follows we shall take the size of the chains to be 200 segments, typical of proteins, with each block comprising 100 monomer units. The chains are tethered to the surface at their hydrophobic end. The solvent is assumed to be a bad solvent, $\chi_{A\sigma}=\chi_{C\sigma}=1$ (in units of $k_BT$), for the hydrophobic segments of both the diblocks polymer and the surfactant. Similarly, for the hydrophilic monomers of both molecules, i.e. segment types B and D, the solvent is considered to be athermal (i.e. a good solvent, $\chi_{B\sigma}=\chi_{D\sigma}=0$). The Flory-Huggins parameters for all the interactions between hydrophobic and hydrophilic segments are set to 1. While the hydrophilic monomers (B) and (D) have no affinity to adsorb onto the solid interface, the adsorption energy of hydrophobic segments (A) and (C), per monomer unit, are taken as –1 and –2.5 (in units of $k_BT$), respectively. Lastly, but most crucially, we assume $\chi_{AC}=2.5$, indicating some degree of incompatibility between the adsorbing segments of the macromolecule and those of the surfactant molecules.

Figure 1 presents the results of the isotherm for the adsorption of the surfactant onto an isolated hydrophobic solid surface, pretreated with a diblock polymer brush as mentioned above. The amount of the macromolecule at the interface is set to 0.005 chains per unit monomer area $(a_0)^2$. The graph shows the value of the excess amount of surfactant per interfacial unit area, defined as

$$\theta_s=\frac{1}{2}\sum_{k=1}^{L}\left(\phi_s(k)-\Phi_s\right) \tag{11}$$

plotted against the bulk volume fraction of surfactant, $\Phi_s$. We obtain the results for an isolated interface by performing the calculations for our two surfaces placed at sufficiently large separations from each other (hence the factor of 0.5 in (11)).

At low values of surfactant bulk volume fraction below $4.35\times10^{-4}$, the amount of excess surfactant at the interface is seen to increase smoothly (solid line) following a typical isotherm for adsorption of such surfactants onto a surface. However, as the bulk volume fraction of surfactant reaches the value $4.35\times10^{-4}$, the amount of excess adsorbed surfactant is found to make a sudden and discontinuous jump to a much higher value, increasing from $\theta_s=0.254$ to 1.320 per monomer unit area, $(a_0)^2$. The location of this abrupt jump is indicated by the arrow in figure 1. For surfactant bulk volume fractions beyond $\Phi_s=4.35\times10^{-4}$, the excess surfactant amount continues to increases smoothly once again. This trend is also closely followed by the volume fraction of surfactant segments in the first layer in direct contact with the solid surface. The graph in figure 2(*a*) shows the variation in the value of $\phi_s(1)$ plotted against the surfactant bulk volume fraction.

As might be expected, associated with a sudden increase in the number of surfactant molecules adsorbed at the interface, there is also an abrupt drop in the volume fraction of the diblocks polymer segments, $\phi_p(1)$, that are in contact with the surface. As is seen in the plot of $\phi_p(1)$ against $\Phi_s$ in figure 3, the drop occurs at precisely the same surfactant bulk volume fraction of $4.35\times10^{-4}$. The change in the value of $\phi_p(1)$, from 0.455 down to a much lower value of 0.01 at this surfactant bulk volume fraction, is interpreted as signalling a sudden change in the conformation of the chains, from originally having their hydrophobic blocks lying relatively flat on the surface to ones which now protrude away some distance into the bulk solution.

The abrupt changes in the amount of adsorbed surfactant and the associated changes in the number of biopolymer segments in contact with the surface are reminiscence of the existence of a first-order phase transition in these layers, somewhat similar to those already predicted for pure ionic surfactant systems under certain circumstances [53, 54]. One of the most notable features of any first-order phase transition is the existence of metastable states. Such metastable states should be easily detectable by the numerical scheme presented in the previous section. As mentioned previously, the method can converge to solutions representing local free energy minimums. We investigated such a possibility, by starting our calculations with a large number of initial guess values for the set of auxiliary fields $\{\psi^{\alpha}(k)\}$. Close to the surfactant bulk volume fraction at which the transition is observed, we indeed find that for some of these initial starting values, the calculations converge to a secondary solution different to the one shown by solid lines in figures 1 and 2. The corresponding values of $\theta_s$, $\phi_s(1)$ and $\phi_p(1)$ for these secondary solutions are shown as dashed lines in each of the three figures, respectively. It is noticeable that these additional solutions form the continuation of the solid lines on each side of the transition point. Furthermore, the free energy associated with these secondary solutions is always higher than the one calculated for the stable ones shown by the solid lines. From now on, we shall refer to the two distinct branches of the curves in figures 1 and 2, as the low surfactant coverage (LSC) and the high surfactant coverage (HSC) phases. Thus, the solutions for each phase, shown by the dashed lines, essentially constitute parts of a van

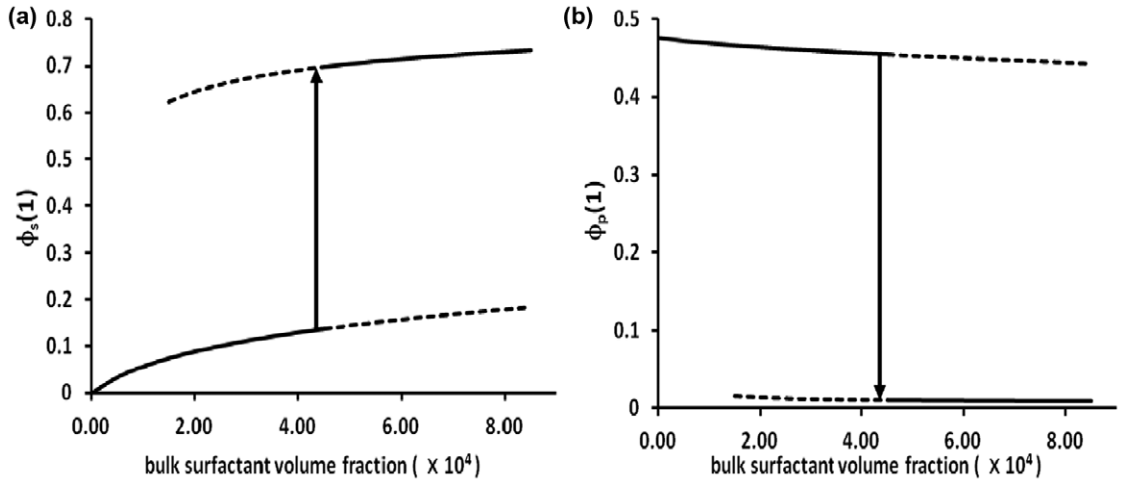


**Figure 2.** Variation in the number of contacts between the surface and surfactant monomers (a) monomers belonging to chains (b), plotted against the volume fraction of the surfactant in the bulk solution. Dotted lines indicate the values obtained for the metastable states.

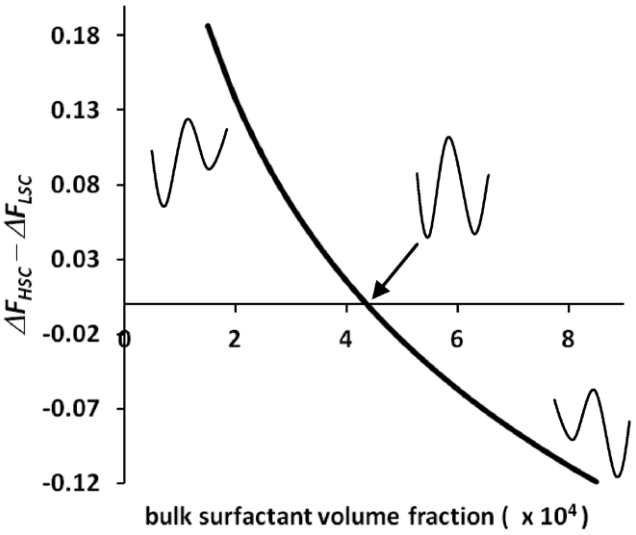


**Figure 3.** The difference in the free energy between the high surfactant and the low surfactant coverage phases, in units of $k_BT/(a_0)^2$, plotted as a function of the bulk surfactant volume fraction.

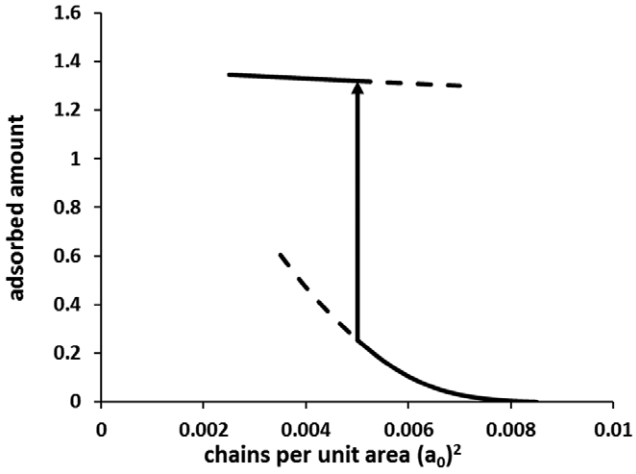


**Figure 4.** The same as figure 1, but now with the bulk surfactant volume fraction kept constant at $4.35\times10^{-4}$, and the number of chains on the surface varied instead.

der Waals loop around the transition point. Using our current method we have not been able to calculate the entire loop, but this has been done in a number of recent studies focusing on transitions in adsorbed single component ionic surfactant layers [53, 54]. However, the transition in these systems has a very different driving force resulting from the interplay between the formation of bilayers and the electrostatic forces between the interfacial adsorbed films.

The existence of a first-order phase transition in the above mixed surfactant + diblock polymer layers can be further verified by considering the changes in the free energy difference between the high and the low surfactant coverage phases, as the bulk concentration of the surfactant is varied. Using (10), the free energy for each phase was determined and the difference, in units of $k_BT(a_0)^{-2}$, is plotted against the surfactant bulk volume fraction in figure 3. The graph clearly shows that at the transition point, corresponding to a bulk surfactant volume fraction of $4.35\times10^{-4}$, the difference between the free energy of the two phases becomes zero. This is much as one would expect. Below this value, the HSC phase has a higher free energy and therefore constitutes a metastable state. Above the surfactant bulk concentration corresponding to the transition on the other hand, the high surfactant coverage phase has a lower free energy and it is now the LSC phase that is the metastable state. This result further supports the presence of a first-order phase transition in such a mixed biopolymer + surfactant system, with the difference in the excess amount of surfactant at the interface for the two phases providing a possible measure of the order parameter for the transition. Schematics for the variation of the free energy with this order parameter, displaying the metastability, are included in figure 3 at both sides of the transition point. The maxima in these diagrams are also stationary points. Therefore, using the implementation of the SCF method presented in section 2, it should be possible in principle to locate them. While we have been able to obtain such maxima for a few examples, in

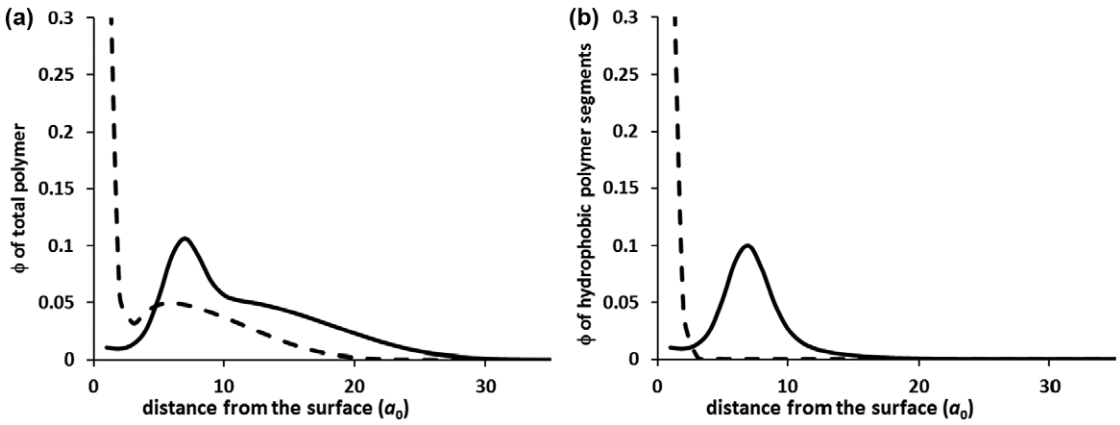


**Figure 5.** Density profile of biopolymer (a) hydrophobic residues of the biopolymer (b), plotted as a function of distance away from the interface, for the LSC (dashed line) and HSC (solid line) phases.

most cases this requires a rather large number of initial guess solutions before some of these converge to the maximum. For the overwhelming majority of these, the stationary solution found is one of either the stable or the metastable minimum. Nonetheless, determination of the energy barrier between the stable and metastable states can be very useful in allowing one to make some predictions regarding the life time of the metastable state and the kinetic time scales for the transitions.

Reported experimental results [5, 6, 14], involving displacement of $\beta$-casein molecules by Tween surfactant at air–water interface, shows some evidence of possible nucleation and growth of surfactant islands within the protein film. During such displacement, it is the amount of protein at the interface that gradually changes. It is therefore useful to consider a situation in which the bulk volume fraction of surfactant is maintained at a fixed value while the number of macromolecular chains at the interface is varied. The results for such an exercise are displayed in figure 4, for a system with the same model polymer and surfactant molecules as those of figure 1. The surfactant bulk volume fraction is set to $\Phi_s = 4.35\times10^{-4}$. With a relatively high number of polymers at the interface, the amount of adsorbed surfactant is quite small. As the number of chains decreases, the value of $\theta_s$ increases smoothly at first. However, once the coverage of chains reaches the transition value of 0.005 chains per monomer unit area $(a_0)^2$, the amount of surfactant adsorbed at the interface shows an abrupt increase from a value of 0.254 to a much higher value of 1.320. At the same time, the number of contacts between the biopolymer chains and the solid surface is reduced from 0.455 down to 0.010 contacts per unit monomer area. As before, in figure 4 we have also shown some parts of the van der Waals loops around the transition point corresponding to the metastable states. These are represented by the dotted lines in the graph.

The results obtained here indicate that the displacement of protein molecules at interfaces can be accompanied by a configurational and structural phase transition in the interfacial layer, whereupon there can be a sudden uptake of surfactant once the amount of displaced polymer reaches the transition value. This can manifest itself as nucleation and growth of the HSC phase domains within the LSC phase. Some evidence for this behaviour seems to be provided by the AFM images during the displacement of $\beta$-casein molecules by the non-ionic surfactant Tween 20. These show the formation of near-circular surfactant-rich domains, from which the biopolymer has been displaced, within the protein film [5, 6, 14]. Furthermore, phase transition behaviour of this type can also lead to emergence of phase separated regions, resulting in a heterogeneous film, if the amphiphilic macromolecules possess some degree of lateral mobility. In this work the kinetics of the formation and growth of such domains has not been considered. Instead the focus is on calculating the properties of the initial (metastable) and the final (equilibrium) states, both of which are assumed to be laterally homogeneous. The possibility of combining the present model with our previous one [18] to account for such mobility and kinetics of phase separation will be investigated in a future study. It is interesting to note that, where the bonds between protein molecules are stronger and closer to being irreversible, the displacement kinetics becomes entirely different, as has been demonstrated by experiments involving $\beta$-lactoglobulin and surfactants [7, 10, 11] and our own Brownian dynamic simulations [14, 15].

### 3.2. Segment density profiles

The phase transition in the macromolecular brush layer, induced by the adsorption of the surfactant molecules, involves substantial changes in the conformation of the chains at the interface. Useful information on the configurations adopted by the chains can be inferred by studying the variation of the density profile of biopolymer and surfactant molecules within the mixed interfacial layer.

The graph in figure 5(*a*) presents the density profile of the anchored chains, plotted as a function of the distance away from the solid surface. The profiles shown are for the high surfactant coverage (solid line) and the low surfactant coverage (dashed line) phases, both at the bulk concentration corresponding to the transition point. Although the surface free energies associated with both of these profiles are identical, it is seen that the two are markedly different. The chains in the HSC phase are significantly more stretched into the bulk

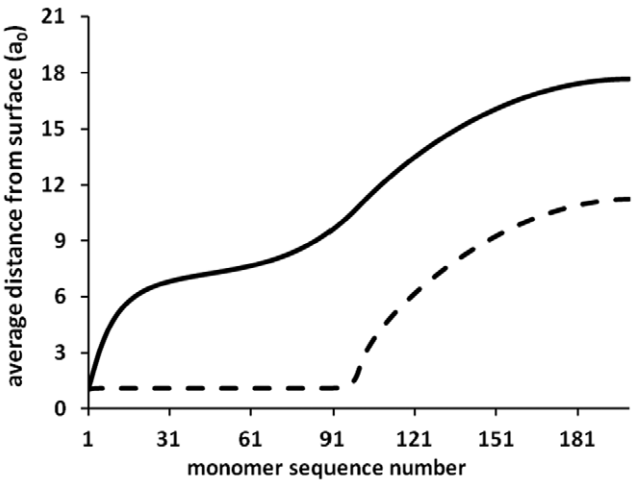


**Figure 6.** The average distance away from the surface for each monomer of the tethered chain. Monomers are numbered sequentially from 1 to 200, starting with the anchored end. The solid line shows the results for the HSC and the dashed line for the LSC phases, both at the transition point.

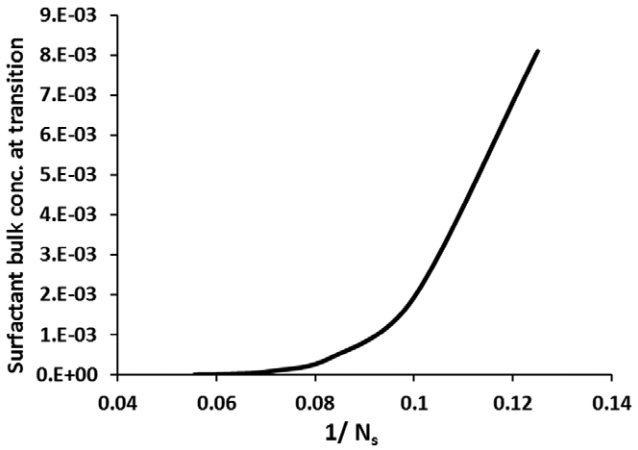


**Figure 7.** The bulk surfactant volume fraction at which the transition from LSC to HSC phases occurs, plotted as a function of the inverse surfactant size.

solution. In turn, this is expected to give rise to longer range interactions between two surfaces covered with such biopolymers, when the chains adopt the configurations in the HSC phase. We shall discuss this point later. In the case of the low surfactant coverage phase, the concentration of the polymer increases significantly as one approaches the solid surface. On the other hand, for the high surfactant coverage phase, the polymer density at the solid surface is much lower, with a maximum now occurring at a distance of around 7 monomer units away from the surface. Almost all the segments belonging to macromolecules that reside in this peak belong to the hydrophobic parts of the chains. This can more clearly be seen from the solid curve in figure 5(*b*), where we have now only included the variation of the density of the hydrophobic segments of the diblocks polymer chains. We stress again that the displacement of the hydrophobic segments of the polymer by the surfactant is in itself not surprising; indeed it is very much expected. However, what is interesting here is the possibility of a first-order phase transition, and the associated metastability, during the process.

Further information on the configurations adopted by chains may also be obtained by considering the average distance $<R_i>$ of each segment away from the solid surface. Figure 6 shows such a graph. The segments have been numbered consecutively along the chain backbone, starting from the hydrophobic segment attached to the surface. Once again, the solid line represents the results for the HSC and the dashed line those for the LSC phases. In the low surfactant coverage phase the hydrophobic parts of the biopolymer lie very flat on the surface. For the HSC phase, a large portion of these hydrophobic segments now reside at a distance of around 7 monomer units, consistent with the peak seen in figures 5(*b*). The more extended nature of the chains in the HSC phase is also evident from these graphs. At the transition point, the average distance of the free ends of the chains away from the surface changes from a value of $<R_i> = 11.2a_0$ up to $<R_i> = 17.6a_0$.

We note here that some of the main features of the results described above were presented in preliminary form in a published conference report [68]. These previous calculations were based on a slightly different model system with the surfactant species comprising 2 head and 2 tail segments and with different assumed values of the various Flory-Huggins parameters.

### *3.3. Variation of the transition point with system dependent parameters*

The transition in the adsorption behaviour of surfactant molecules studied in the previous section is focused on a particular surfactant size, polymer architecture and strength of unfavourable interactions between the two species. In order to establish the generality or otherwise of the transition behaviour, in this section we examine how sensitive such behaviour is to the variation in one of these parameters.

We consider the surfactant size dependence of the transition point. It is known that larger amphiphilic molecules tend to have a higher affinity for interfacial adsorption at lower bulk concentrations, when compared to smaller surfactants. This is despite the fact that normally they have a lower maximum surface coverage at high bulk concentrations than latter. It is for this reason that, at higher concentrations, such large macromolecules are displaced by lower molecular weight surfactants. Therefore, one may expect that the transition in the surfactant adsorption isotherms should occur at even lower bulk concentrations, as the size of the surfactant molecules is increased. This is indeed what is predicted by our SCF calculations. In figure 7 we present the bulk surfactant concentration at which the transition occurs, plotted against the inverse surfactant size, for a range of surfactant sizes from 4 to 18. We have kept the number of hydrophobic and hydrophilic segments of the surfactant equal to each other for all sizes. Also the interaction parameters are identical to those used in previous sections, with the surface coverage of macromolecules set once again to 0.005 chains per area $(a_0)^2$.

From figure 7 it is not entirely obvious whether the transition concentration continues to decrease indefinitely as the

number of hydrophobic and hydrophilic residues of the surfactant are increased ($N_s \to \infty$). It could also be the case that at some finite size value the transition ceases altogether. If so, this point may be a critical point for the transition studied here. The existence of a critical point is more likely if one considers the variation of the surfactant bulk volume fraction at the transition, with the degree of the incompatibility $\chi$ between the adsorbing groups of the diblocks polymer and the surfactant. However, we leave the investigation of this interesting problem to a future publication. Suffice it to say here that, as the strength of unfavourable interactions between the surfactant and biopolymer is reduced, the gap in the adsorption isotherms of figures 1, 2 and 4 will become smaller. Taking the difference in the surfactant coverage between the two phases as the order parameter, one sees that this is likely to vanish at some given value of $\chi$. This value of $\chi$ then constitutes a critical point. As with all critical phenomena, we expect that the fluctuations (in the amount of adsorbed surfactant molecules here) to become large at the critical point. Therefore, it is also likely that close to the critical point, our mean-field SCF calculations cease to become valid and a resort to other techniques has to be made.

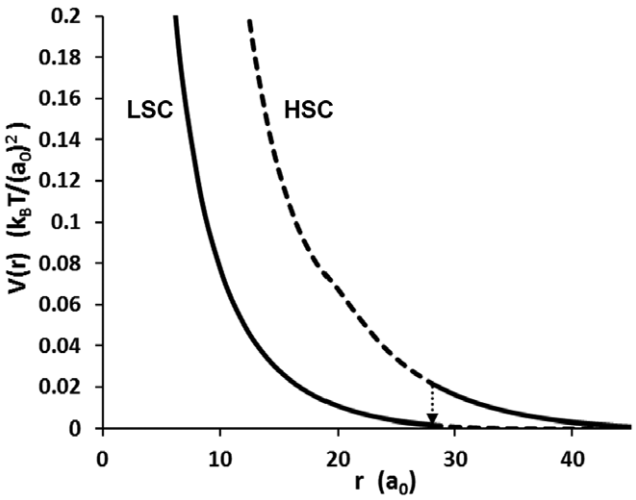


**Figure 8.** Interaction potential per unit area, mediated by the overlap of biopolymer + surfactant films, plotted against the surface separation distance, for layers in both the HSC and LSC phases. The dashed part of each curve shows the range of separations for which the corresponding phase is a metastable state.

## 4. Interaction between two surfaces

So far, our discussions have solely focused on the adsorption of surfactant onto a single isolated interface. For two surfaces approaching each other, another parameter that could also induce a transition is the separation distance between the interfaces. To investigate this aspect, we consider a system with a bulk surfactant concentration slightly above the transition value in figure 1. Then, at large separations, the equilibrium configuration of the chains will be a stretched out one similar to that shown as the solid line in figure 6. This allows for the high surface coverage of the interface by the surfactant. However, as the plates are moved closer and the extended macromolecular layers begin to overlap, it is likely that a transition to the lower surfactant surface coverage phase will take place, causing the hydrophobic sections of the chains to lie flat on the surfaces and the chains to become less stretched (see the dotted line in figure 6). This in turn reduces the degree of overlap between the chains. Thus, while for this system at large separations the HSC phase has the lower free energy, one expects that at closer distances the LSC phase will become the equilibrium state. In other words there will be a distance at which both phases will have equal free energy. This surface separation is the transition point.

To test this idea we have calculated the value of the free energy for the density profiles that result from the procedure described in section 2. This was done at various plate separation distances. We used a system with a biopolymer surface coverage of 0.005 chains per unit area $(a_0)^2$ and a bulk surfactant volume fraction $\Phi_s = 5\times10^{-4}$, marginally above the transition value of $4.35\times10^{-4}$ reported in section 3.1. At all gap sizes we found more than one free energy minimum, with one of these possessing the lowest free energy value, thus being the stable phase, and the other constituting a metastable state. It was noticed that at a finite surface separation of ~ $28a_0$, the calculated free energy values of HSC and LSC phases crossed over, with the low surfactant coverage phase becoming the stable phase for smaller gap sizes, while the HSC being the equilibrium state at larger distances. A phase transition induced by confinement has also been observed in the SCF calculations of Leermakers *et al* [53, 54], involving the adsorption in somewhat different systems, consisting only of pure ionic surfactant. As these studies have highlighted, the existence of the phase transition and metastable states can lead to hysteresis loops for such systems in the force–distance curves, as e.g. obtained by AFM. We have calculated the interactions induced by the overlap of biopolymer + surfactant layers both in HSC and LSC phases using $V(r) = \Delta F(r) - \Delta F(\infty)$. The free energies $\Delta F(r)$ and $\Delta F(\infty)$ are calculated according to (10) for each of the two phases, at plate separations $r$ and at a suitably large distance where the value of $\Delta F$ no longer changes with the gap size. The interaction potential for each phase, throughout the whole separation range considered, was obtained irrespective of whether it was the stable or the metastable state. The variation of the interaction potential per unit area (in units of $(k_BT/(a_0)^2)$, plotted against the separation distance (in units of monomer size $a_0$), is displayed in figure 8, for both of the phases. In both cases the interactions are purely repulsive as may be expected given the diblock nature of our model protein. However, it is quite clear that the magnitude and the range of the repulsive forces are quite different for the two cases, being distinctly longer ranged and stronger for the HSC phase. Again, this is not unexpected, since as we have seen previously (figure 6) in the high surfactant coverage phase, the diblocks polymer chains protrude much further into the solution and away from the interfaces.

For each curve in figure 8 we have highlighted the range of values of $r$ for which the corresponding phase is a metastable phase using dashed lines. Thus, an AFM experiment,

done extremely slowly so as to keep the layers at equilibrium at all times, would be expected to follow the solid line with an abrupt change occurring at a gap size of $28a_0$. In practice, and depending on the height of the energy barrier between the two phases, one expects that the sudden change would occur at some distance less than this gap size for the inward sweep and at a higher value for the outward one, giving rise to the possibility of hysteresis in the measured force–distance curves.

We finish this section by cautioning that a more exhaustive search, involving a much larger number of initial starting guess solutions in our SCF calculations, may reveal a larger number of metastable states and a rougher free energy landscape than the one found here. In particular, in future studies, the possibility of a non-symmetric phase needs to be explored. In such a case, the adsorbed amount of surfactant on the two plates need not necessarily be the same, with the likelihood that the broken symmetric phase may even become the lower free energy ground state.

## 5. Conclusions

Protein and surfactant molecules are invariably found together in many food colloid formulations. We have argued that, during the competitive displacement of protein by the surfactant from the interfaces, the amount of protein on the surface varies slowly, whereas the kinetics of adsorption/desorption of the surfactant is much faster. Thus, one may consider the system as one with a fixed number of macromolecules residing on the interface at any given time, with the surfactant coverage on this biopolymer laden surface being in equilibrium with the bulk solution. We show, by means of numerical SCF calculations that, where there is a strong degree of incompatibility between the adsorbing parts of the biopolymer and the surfactant molecules, the equilibrium adsorbed amount of the surfactant shows an abrupt change as the coverage of the interface by the biopolymer chains is reduced. This sudden transition also manifests itself in the adsorption isotherm for the surfactant, where the number of amphiphilic macromolecules is kept fixed and the bulk surfactant concentration is varied instead. Although direct unfavourable interactions between proteins and certain surfactants, such as fluorinated surfactants [23], can in principle be engineered, we believe that a more common possibility involves protein molecules capable of forming reversible bonds amongst themselves. These bonds need to be sufficiently strong to produce a reasonable degree of incompatibility, while still remaining reversible so as not to trap the structure and hinder the lateral movement of the chains [17]. In our previous work using both theoretical calculations and Brownian dynamics simulations [17, 27] we had shown the possibility of both bulk and surface phase separation, resulting from the presence of such reversible bonds between one set of molecules but not the other, in systems consisting of a mixture of the two.

We demonstrate that the abrupt change in the amount of adsorbed surfactant is the result of a first-order phase transition in the system. Using SCF calculations, we have also been able to locate the metastable states associated with this transition, and therefore the parts of the van der Waals loop around the transition point. We find that, as is expected for a first-order phase transition, the free energy of the stable and the metastable state approach each other as the surfactant bulk concentration corresponding to the transition is approached. At the transition point, the two free energies become equal and then exhibit a crossover. We identify the stable and the metastable states as surfactant + macromolecule films having high surfactant surface coverage (HSC) and low surfactant surface coverage (LSC) configurations. It is shown that the separation distance itself can act as another possible parameter, capable of inducing the phase transition. In particular, while in the same system the HSC phase can be the minimum free energy state when the surfaces are far apart, at closer separations the LSC becomes the equilibrium state. Once again the transition between the two film structures occurs abruptly at a transition gap size. The very different conformation of the diblocks polymer chains in these two states produces significantly different steric colloidal interaction potentials when two such adsorbed layers overlap. Depending on the height of the energy barrier between the HSC and LSC phases, and the duration of the experiment, a hysteresis in the force versus separation distance graph is predicted, much in the same way as has been calculated for certain pure ionic surfactant systems [53, 54].

A possible practical application of the phase transition phenomenon described in this study is in the development of a ‘smart’ responsive colloid. In a suitably designed dense colloidal dispersion or emulsion, the occurrence of an interfacial first-order transition of the type described here could induce a substantial change in the effective particle volume fraction or the state of particle aggregation. This might then lead to a sudden jump in the system’s bulk rheological behaviour, as reflected in the transformation from a low-viscosity state to a solid gel-like state. Such a sudden jump in macroscopic properties could therefore be induced by the addition of a very small amount of extra surfactant to the system. Additionally, in a dispersion containing adsorbed polyelectrolyte, the exact position of the phase transition point is likely to be highly sensitive to solution thermodynamic variables such as temperature or pH. Hence it is possible to envisage that a small change in temperature or pH of a mixed surfactant/biopolymer colloidal system, under conditions lying close to the interfacial phase transition point, could also trigger a dramatic change in its rheological and textural properties. This corresponds to the behaviour of an environmentally responsive colloid.

The current exploratory study has highlighted the rich variety of behaviour in these types of biopolymer + surfactant films. Further theoretical studies to determine the behaviour of the system near the critical point, as well as a fuller picture of the free energy landscape of these layers, particularly when confined between two surfaces, remain interesting problems for future research. It would also be useful to study the same system using a slightly different model more amenable to direct analytical calculations. An example of such a model might be the one developed by Fainerman *et al* [8, 16, 69], where the states of the adsorbed protein chains are represented by a relatively small number

of configurations, each occupying a different surface area. This model was used to study the kinetic and equilibrium properties of surfactant + protein layers where the association between the two species was synergistic. We suspect that the same model could also be used to study situations where the interaction between the competing surfactant and biopolymer is an unfavourable one. Similarly, careful experimental studies involving AFM force measurements, to investigate the possibility of hysteresis, and Brewster angle microscopy to probe the changing structure of the mixed layers, might provide more direct evidence for the existence and nature of the phase transition behaviour predicted for the interfacial films studied here.

## Acknowledgments

We gratefully acknowledge many useful discussions with Professor Jianshe Chen and Dr Anna Akinshina.

## References

[1] Dickinson E 1992 *An Introduction to Food Colloid* (Oxford: Oxford University Press)
[2] Dickinson E 2011 *Food Hydrocolloid* **25** 1966–83
[3] Hasenhuettl G L and Hartel R W 1997 *Food Emulsifiers and Their Applications* (New York: Chapman and Hall)
[4] Dickinson E 2013 *J. Sci. Food Agric.* **93** 710–21
[5] Gunning P A, Mackie A R, Gunning A P, Wilde P J, Woodward N C and Morris V J 2004 *Food Hydrocolloid* **18** 509–15
[6] Mackie A R, Gunning A P, Wilde P J and Morris V J 1999 *J. Colloid Interface Sci.* **210** 157–66
[7] Gunning P A, Mackie A R, Gunning A P, Woodward N C, Wilde P J and Morris V J 2004 *Biomacromolecules* **5** 984–91
[8] Miller R, Fainerman V B, Leser M E and Michel M 2004 *Curr. Opin. Colloid Interface Sci.* **9** 350–6
[9] Miller R, Leser M E, Michel M and Fainerman V B 2005 *J. Phys. Chem.* B **109** 13327–31
[10] Mackie A R, Gunning A P, Pugnaloni L A, Dickinson E, Wilde P J and Morris V J 2003 *Langmuir* **19** 6032–8
[11] Mackie A R, Gunning A P, Ridout M J, Wilde P J and Morris V J 2001 *Langmuir* **17** 6593–8
[12] Mackie A R, Gunning A P, Wilde P J and Morris V J 2000 *Langmuir* **16** 8176–81
[13] Woodward N C, Gunning A P, Mackie A R, Wilde P J and Morris V J 2009 *Langmuir* **25** 6739–44
[14] Pugnaloni L A, Dickinson E, Ettelaie R, Mackie A R and Wilde P J 2004 *Adv. Colloid Interface Sci.* **107** 27–49
[15] Pugnaloni L A, Ettelaie R and Dickinson E 2003 *Colloids Surf.* B **31** 149–57
[16] Fainerman V B, Zholob S A, Leser M, Michel M and Miller R 2004 *J. Colloid Interface Sci.* **274** 496–501
[17] Pugnaloni L A, Ettelaie R and Dickinson E 2003 *Langmuir* **19** 1923–6
[18] Pugnaloni L A, Ettelaie R and Dickinson E 2004 *J. Chem. Phys.* **121** 3775–83
[19] Hunter R J 2000 *Foundations of Colloid Science* (Oxford: Clarendron)
[20] Lyklema J 1991 *Fundamentals of Interface and Colloid Science: Fundamentals* vol 1 (New York: Academic)
[21] Shull K R 1993 *Macromolecules* **26** 2346–60
[22] Bernardini C, Stuart M A C, Stoyanov S D, Arnaudov L N and Leermakers F A M 2012 *Langmuir* **28** 5614–21
[23] Essalhi M and Khayet M 2012 *J. Membr. Sci.* **417** 163–73
[24] Reister E, Muller M and Kumar S K 2005 *Macromolecules* **38** 5158–69
[25] Prasad S, Zhu H, Kurian A, Badge I and Dhinojwala A 2013 *Langmuir* **29** 15727–31
[26] Affrossman S, Kiff T, O'Neill S A, Pethrick R A and Richards R W 1999 *Macromolecules* **32** 2721–30
[27] Annable T and Ettelaie R 1994 *Macromolecules* **27** 5616–22
[28] Annable T and Ettelaie R 1996 *J. Chim. Phys. Phys.-Chim. Biol.* **93** 899–919
[29] Jimenez-Regalado E, Selb J and Candau F 2000 *Macromolecules* **33** 8720–30
[30] Annable T, Buscall R and Ettelaie R 1996 *Colloids Surf.* A **112** 97–116
[31] Razumovsky L and Damodaran S 1999 *Colloid Surf.* B **13** 251–61
[32] Razumovsky L and Damodaran S 2001 *J. Agric. Food Chem.* **49** 3080–6
[33] Sengupta T and Damodaran S 2001 *J. Agric. Food Chem.* **49** 3087–91
[34] Damodaran S 2004 *Curr. Opin. Colloid Interface Sci.* **9** 328–39
[35] Damodaran S and Rao C S 2001 *Food Colloids: Fundamentals of Formulation*, ed E Dickinson and R Miller (Cambridge: Royal Society of Chemistry) pp 165–80
[36] Dickinson E 1999 *Colloid Surf.* B **15** 161–76
[37] Dickinson E 1998 *J. Chem. Soc. Faraday Trans.* **94** 1657–69
[38] Dan A, Wuestneck R, Krägel J, Aksenenko E V, Fainerman V B and Miller R 2014 *Food Hydrocolloids* **34** 193–201
[39] Maldonado-Valderrama J, Fainerman V B, Aksenenko E, Galvez-Ruiz M J, Cabrerizo-Vilchez M A and Miller R 2005 *Colloids Surf.* A **261** 85–92
[40] Ramirez P, Munoz J, Fainerman V B, Aksenenko E V, Mucic N and Miller R 2010 *Colloids Surf.* A **391** 119–24
[41] Miller R, Grigoriev D O, Krägel J, Makievski A V, Maldonado-Valderrama J, Leser M, Michel M and Fainerman V B 2005 *Food Hydrocolloids* **19** 479–83
[42] Makievski A V, Miller R, Czichocki G and Fainerman V B 1998 *Colloids Surf.* A **133** 313–26
[43] Rosen M J and Song L D 1996 *J. Colloid Interface Sci.* **179** 261–8
[44] Chang C H and Franses E I 1992 *Colloids Surf.* **69** 189–201
[45] Scheutjens J and Fleer G J 1979 *J. Phys. Chem.* **83** 1619–35
[46] Scheutjens J and Fleer G J 1980 *J. Phys. Chem.* **84** 178–90
[47] Fleer G J, Cohen Stuart M A, Scheutjens J M H M, Cosgrove T and Vincent B 1993 *Polymers at Interfaces* (London: Chapman and Hall)
[48] Milner S T 1991 *Science* **251** 905–14
[49] Leermakers F A M and Egorov S A 2013 *Soft Matter* **9** 3341–8
[50] Currie E P K, Leermakers F A M, Stuart M A C and Fleer G J 1999 *Macromolecules* **32** 487–98
[51] Bray A J and Moore M A 1984 *J. Phys. C* **17** L463–8
[52] Skvortsov A M, Gorbunov A A, Leermakers F A M and Fleer G J 1999 *Macromolecules* **32** 2004–15
[53] Koopal L K, Leermakers F A M, Lokar W J and Ducker W A 2005 *Langmuir* **21** 10089–95
[54] Leermakers F A M, Koopal L K, Lokar W J and Ducker W A 2005 *Langmuir* **21** 11534–45
[55] Ferreira P G and Leibler L 1996 *J. Chem. Phys.* **105** 9362–70
[56] Grosberg A Y and Khokhlov A R 1994 *Statistical Physics of Macromolecules* (New York: AIP)
[57] Fredrickson G H, Ganesan V and Drolet F 2002 *Macromolecules* **35** 16–39
[58] Scheutjens J and Fleer G J 1985 *Macromolecules* **18** 1882–900
[59] Evers O A, Scheutjens J and Fleer G J 1990 *Macromolecules* **23** 5221–33

[60] Evers O A, Scheutjens J and Fleer G J 1991 *Macromolecules* **24** 5558–66
[61] Ettelaie R, Khandelwal N and Wilkinson R 2014 *Food Hydrocolloids* **34** 236–46
[62] Ettelaie R, Murray B S and James E L 2003 *Colloid Surf.* B **31** 195–206
[63] Lyklema J 2005 *Fundamentals of Interface and Colloid Science*, ed J Lyklema (San Diego: Academic) pp 1–12
[64] Mezzenga R, Lee W B and Fredrickson G H 2006 *Trends Food Sci. Technol.* **17** 220–6
[65] Mezzenga R, Ruokolainen J, Fredrickson G H and Kramer E J 2003 *Macromolecules* **36** 4466–71
[66] de Kruif C G and Zhulina E B 1996 *Colloids Surf.* A **117** 151–9
[67] Mellema M, Leermakers F A M and de Kruif C G 1999 *Langmuir* **15** 6304–13
[68] Ettelaie R, Dickinson E, Cao L and Pugnaloni L A 2007 *Food Colloids: Self-Assembly and Material Science*, ed E Dickinson and M E Leser (Cambridge: Royal Society of Chemistry) pp 245–56
[69] Fainerman V B, Zholob S A, Lucassen-Reynders E H and Miller R 2003 *J. Colloid Interface Sci.* **261** 180–3